

# Calibration for Single-Carrier preFDE Transceivers Based on Property Mapping Principles

M. Petermann, D. Wübben, A. Dekorsy, K.-D. Kammeyer

Department of Communications Engineering

University of Bremen, 28359 Bremen, Germany

Email: {petermann, wuebben, dekorsy, kammeyer}@ant.uni-bremen.de

**Abstract**—In general, the unequal RF circuitry in the transmit and receive chains at the base station (BS) prevents the exploitation of the uplink (UL) channel estimate for proper pre-equalization in time division duplex (TDD) systems. To avoid additional transceiver hardware costs for matching networks, the idea of relative calibration was introduced to cope with the different effective channel impulse responses of UL and downlink (DL) by means of signal processing. However, multiple-input multiple-output (MIMO) transmission in frequency-selective channels does not allow for classical frequency-domain calibration principles based on total least squares (TLS) approaches. Consequently, more complex structured total least squares (STLS) problems must be solved.

In this paper the application of the signal property mapping principle is introduced to iteratively solve the STLS calibration problem. Exemplified by simulation results for single-carrier frequency-domain pre-equalization (SC-preFDE) systems the algorithm indicates good and fast convergence behavior and effectively exploits noisy UL and DL channel measurements for system calibration.

## I. INTRODUCTION

The trend of modern wireless communication systems is to shift the complexity from the mobile terminals to the base station (BS), thus to enable low-cost and low-power mobile stations (MS). Hence, pre-equalization strategies are widely studied, especially for multi-carrier systems in time division duplex (TDD) mode as the channel state information (CSI) from the uplink (UL) can be used for pre-processing at the BS prior to downlink (DL) transmission [1]. Therefore, the direct utilization of uplink CSI in baseband pre-processing necessitates channel reciprocity [2]. However, due to transceiver front-end design requirements, e.g., different amplifiers and radio frequency (RF) components as well as time-variant effects due to, e.g., temperature and humidity, non-symmetric characteristics in the analog transmit (Tx) and receive (Rx) front-ends annihilates the reciprocal property of the effective channels and cause severe interference especially in space division multiple access (SDMA) schemes [3] and in cooperative transmission [4]. In new low-cost wireless transceivers, a current paradigm shift is to accept the existing impairments and to mitigate the effects by additional digital baseband processing or by means of additional low-cost hardware matching networks [5], [6]. To avoid additional hardware solutions, the calibration in signal space, also known as *relative calibration*,

became popular [7]. By establishing a calibration phase during regular transmission with the help of additional feedback, almost equivalent effective UL and DL channels can be recovered. The authors demonstrated the superior performance of the application of such a scheme in comparison with robust pre-equalizer strategies for multicarrier systems [8], [9], where the transceiver influences are assumed to be frequency-independent. There, total least squares (TLS) problems must be solved to acquire estimates of the RF front-end parameters. First ideas to cope with frequency-dependent frequency responses of the RF chains in wideband transmission are given in [10], [11], where the wideband characteristics are handled by calibration on individual frequencies and subsequent interpolation in between. Dealing with this properties solely in time-domain, Guillaud [7], [12] showed that a calibration can be achieved by solving a structured total least squares (STLS) problem. To solve these STLS problems as a generalization in deconvolution problems, several algorithms were presented in the literature [13]–[15].

In this paper, we propose the application of an iterative STLS algorithm for calibration, which maintains the inherent structure of the problem by means of similarity transformations based on the property mapping principle described by Cadzow [16], [17]. The performance of this scheme is demonstrated with a single-carrier system that employs frequency-domain signal processing at the BS for ease of pre-equalizing the frequency-selective channel prior to transmission [1], [18]. This system will be termed single-carrier scheme with frequency-domain pre-equalization (SC-preFDE) in the following. The simulations provide uncoded and coded results for linear pre-equalization and prove significant performance gains at high SNR regions and moderate to high mismatch conditions.

The remainder of this paper is organized as follows. While Sec. II-A deals with the system model that is applied to exemplify the calibration performance, Sec II-B introduces the transceiver influences, which lead to a mismatch between the effective UL and DL channels. Subsequently, the problem formulation is derived in Sec. III-A to resolve the resulting mismatch later on. Then, Sec. III-B provides our solution based on the property mapping principle, followed by Sec. III-C, which gives some comments on the convergence of the proposed algorithm. Simulation results are shown in Sec. IV and, finally, a conclusion is given in Sec. V.

This work was supported in part by the German Research Foundation (DFG) under grant KA 841/21-2

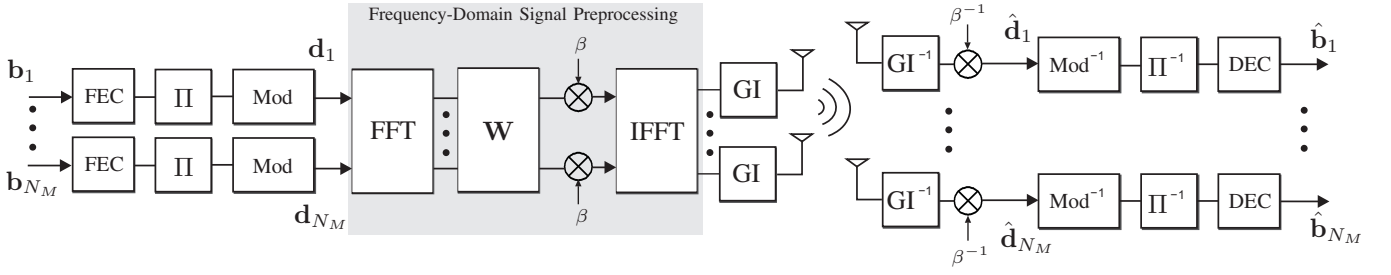


Fig. 1. Frequency-domain joint pre-equalization scheme for a  $N_B \times N_M$  multi-user single-carrier system with block-wise normalization [1]

## II. SYSTEM MODEL

In the subsequent section a general description of the applied system model is presented. Moreover, Sec. II-B deals with the extended channel model that incorporates the non-reciprocity of the effective UL and DL channels.

### A. Single-Carrier System with Pre-Equalization in Frequency-Domain (SC-preFDE)

The application of adaptive transmit strategies in wireless communication systems usually comes along with the need for CSI at the transmitter. If accurate CSI is available, rate and power allocation algorithms or pre-equalization schemes become realizable. It has been shown, e.g., in OFDM systems that low-complexity frequency-domain equalization can be achieved by efficient use of the fast Fourier transform (FFT). To further relieve the mobile receivers from additional complexity, this FFT can be shifted from the mobile stations (MS) towards the BS, which results in a single-carrier scheme with frequency-domain pre-equalization (preFDE) [1]. In addition, the utilization of multiple antennas at the BS allows for SDMA principles such that multiple users (MU) can be served at the same time. Fig. 1 shows the block diagram of such a system. To demonstrate the influence of non-reciprocal channels as described in Sec. II-B and the calibration performance of the proposed algorithm this system will be adopted.

Here, a DL scenario of this system with  $N_B$  base station antennas and  $N_M$  decentralized single-antenna MS is considered, where  $N_B \geq N_M$  should hold. The information bit streams  $\mathbf{b}_j$  of the individual users are separately encoded and interleaved before the encoded bits are modulated to  $M$ -PSK or  $M$ -QAM data symbols  $\mathbf{d}_j$ . These symbol streams are transformed by a FFT of length  $N_c$  to obtain orthogonal samples (or multiple orthogonal MU multiple-input single-output (MISO) systems) in frequency-domain. These samples can be pre-equalized by multiplication with the matrix  $\mathbf{W}$ , which is calculated based on the UL channel estimate of the reverse link in TDD systems. After an inverse FFT (IFFT) a guard interval (GI) of length  $N_g$ , also known as cyclic prefix, is included before upconversion and transmission. At the mobile terminals this cyclic prefix is removed and the received symbols are scaled by the inverse normalization factor  $\beta$ , which has to be signaled to the MSs as side information. Afterwards, the received data symbols  $\hat{\mathbf{d}}_j$  are obtained, which can be demodulated subsequently,

deinterleaved and decoded to yield the estimated bit sequences  $\hat{\mathbf{b}}_j$ . It can be seen clearly that the main complexity has been shifted to the BS.

According to Fig. 1, the mathematical formulation for this scheme can be specified by firstly defining the discrete Fourier transform (DFT) Vandermonde matrix  $\mathbf{F}$  with elements  $[\mathbf{F}]_{m,n} = e^{2\pi jmn/N_c} \equiv \omega^{mn}$  with  $m, n = 0, \dots, N_c - 1$ , where  $\omega$  is a primitive  $N_c$ -th root of unity, and the cyclic prefix matrices  $\tilde{\mathbf{G}}_I$  and  $\tilde{\mathbf{G}}_R$  such that

$$\tilde{\mathbf{G}}_I = \begin{bmatrix} \mathbf{0}_{N_g \times (N_c - N_g)} & \mathbf{I}_{N_g} \\ & \mathbf{I}_{N_c} \end{bmatrix} \quad (1a)$$

$$\tilde{\mathbf{G}}_R = \begin{bmatrix} \mathbf{0}_{N_c \times N_g} & \mathbf{I}_{N_c} \end{bmatrix}. \quad (1b)$$

Then, the following MIMO extensions for the DFT matrix and the insertion and removal of the cyclic prefix can be formulated

$$\mathbf{F}_T = \mathbf{F} \otimes \mathbf{I}_{N_B} \quad (2a)$$

$$\mathbf{G}_I = \tilde{\mathbf{G}}_I \otimes \mathbf{I}_{N_B} \quad \text{and} \quad \mathbf{G}_R = \tilde{\mathbf{G}}_R \otimes \mathbf{I}_{N_M}. \quad (2b)$$

Here,  $\otimes$  being the Kronecker product. Regarding the DFT matrix  $\mathbf{F}_T$ , the matrix  $\mathbf{F}_T^H$  describes the inverse DFT (IDFT) matrix. So, the total system equation for the described single-carrier MU-MISO preFDE scheme at frame  $k$  reads

$$\hat{\mathbf{D}}(k) = \mathbf{G}_R \mathbf{H}(k) \mathbf{G}_I \mathbf{F}_T^H \mathbf{W}(k) \mathbf{F}_T \mathbf{D}(k) + \beta^{-1}(k) \mathbf{N}(k), \quad (3)$$

where  $\mathbf{H}(k)$  is a convolutional block Toeplitz matrix describing the DL channel,  $\mathbf{W}(k) \in \mathbb{C}^{N_B N_c \times N_M N_c}$  is the pre-distortion matrix,  $\mathbf{D}(k) = [\mathbf{d}_1(k), \dots, \mathbf{d}_{N_M}(k)]^T$  comprises all data streams of the users in one frame and  $\mathbf{N}(k)$  is a white Gaussian noise term with variance  $\sigma_N^2$  equal for all samples and users in the frame. The normalization factor  $\beta(k)$  is based on block normalization such that the mean square error of the whole frame is minimized [1]

$$\beta(k) = \sqrt{\frac{N_B N_c}{\text{tr}\{\mathbf{W}(k) \mathbf{W}^H(k)\}}}. \quad (4)$$

Hence, different signal-to-noise ratios for different symbols  $\mathbf{d}_j(k)$  are allowed. Now, by inserting  $\mathbf{F}_T^H \mathbf{F}_T = \mathbf{I}_{N_c}$  in (3) the system equation can be rewritten to

$$\begin{aligned} \hat{\mathbf{D}}(k) &= \mathbf{F}_T^H \mathbf{F}_T \mathbf{G}_R \mathbf{H}(k) \mathbf{G}_I \mathbf{F}_T^H \mathbf{W}(k) \mathbf{F}_T \mathbf{D}(k) + \beta^{-1} \mathbf{N}(k) \\ &= \mathbf{F}_T^H \tilde{\mathbf{H}}(k) \mathbf{W}(k) \mathbf{F}_T \mathbf{D}(k) + \beta^{-1} \mathbf{N}(k). \end{aligned} \quad (5)$$

Consequently, the block-diagonal channel matrix  $\tilde{\mathbf{H}}(k) \in \mathbb{C}^{N_M N_c \times N_B N_c}$  is obtained, which can be efficiently equalized in frequency-domain indicated by the DFT and inverse DFT matrices  $\mathbf{F}_T$  and  $\mathbf{F}_T^H$  multiplied from right and left, respectively. So in order to equalize the DL channel prior to transmission the minimum mean square error (MMSE) filter is applied. Then, the pre-equalization matrix  $\mathbf{W}(k)$  depends on the UL channel estimates of the multi-user MISO channel describable by the block-diagonal matrix  $\tilde{\mathbf{G}}(k) = \mathbf{F}_T \mathbf{G}_R \hat{\mathbf{G}}(k) \mathbf{G}_I \mathbf{F}_T^H$ . The block Toeplitz matrix  $\hat{\mathbf{G}}(k)$  is assumed to be perturbed by errors due to the UL channel estimation. It is modeled by a MMSE error model with constant estimation error variance  $\sigma_e^2$  [9]. Accordingly, this results in

$$\mathbf{W}(k) = \tilde{\mathbf{G}}^H(k) \left( \tilde{\mathbf{G}}(k) \tilde{\mathbf{G}}^H(k) + \sigma_e^2 \mathbf{I}_{N_M} \right)^{-1}. \quad (6)$$

As long as  $\tilde{\mathbf{G}} = \tilde{\mathbf{H}}$  is not fulfilled this choice of the pre-equalization filter matrix leads to undesired multi-user interference due to inappropriate instantaneous effective DL channel CSI.

### B. Transceiver Influences and Reciprocity Model

As already mentioned, the transmit signal experiences a different effective channel during downlink transmission as compared to the uplink transmission due to non-symmetric characteristics of the transceiver front-ends. To include these characteristics into the channel model, a linear reciprocity model for TDD systems as in [7] is assumed. In the remainder of this section the frame index  $k$  is omitted.

Fig. 2 shows this model in time-domain for the single-antenna case. Each direction experiences the same physical reciprocal channel  $\mathbf{p}(t)$  at time  $t$  with a length of  $L_p$  samples, which may contain different delay spreads resulting in longer impulse responses. Here, the presumption that all receive antennas experience the same channel length from all transmit antennas is set. The impulse responses of the transceiver  $\underline{\mathbf{T}}x$

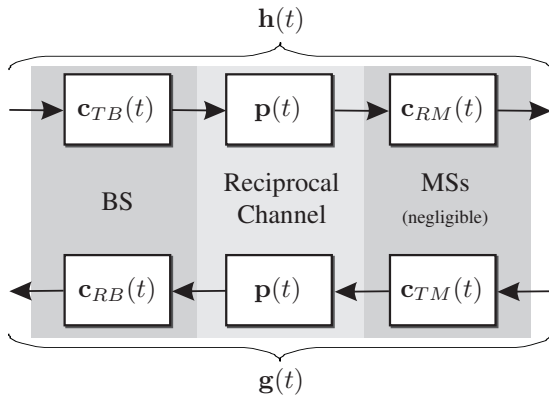


Fig. 2. Non-reciprocity channel model in time-domain for the single-antenna case

and  $\underline{\mathbf{R}}x$  chains are depicted by the filters  $\mathbf{c}_{[T/R]B}(t)$  at the BS and  $\mathbf{c}_{[T/R]M}(t)$  at the mobile stations. Without loss of generality, it was shown that the receiving end does not play

a significant role in adaptive transmit schemes and, thus, can be neglected in further considerations [3]. While the signal in the DL is influenced by  $\mathbf{c}_{TB}(t)$ , the uplink signal is effected by  $\mathbf{c}_{RB}(t)$ , which leads to interference if  $\mathbf{c}_{TB}(t) \neq \mathbf{c}_{RB}(t)$  holds. In case of no coupling effects at the BS the considered MU-MISO system from Sec. II-A consists of  $N_M$  different MISO systems that need to be calibrated.

Mathematically, the impulse responses that are contained in the matrices  $\hat{\mathbf{G}}(k)$  and  $\hat{\mathbf{H}}(k)$  for each Tx-Rx antenna pair  $i, j$  [7]

$$\hat{\mathbf{g}}_{i,j}(t) = \mathbf{p}_{i,j}(t) * \mathbf{c}_{RB,i}(t) \in \mathbb{C}^{L_g} \quad (7a)$$

$$\hat{\mathbf{h}}_{i,j}(t) = \mathbf{p}_{i,j}(t) * \mathbf{c}_{TB,i}(t) \in \mathbb{C}^{L_h} \quad (7b)$$

describe the estimated (accentuated by a  $\hat{\cdot}$ -indication) impulse responses of the system in both directions, where  $\mathbf{p}_{i,j}(t) \in \mathbb{C}^{L_p}$  is the physical reciprocal channel between transmit antenna  $i$  and receive antenna  $j$  and  $\mathbf{c}_{[T/R]B,i}$  are the impulse responses of the BS transmit and receive RF chains [7].

Due to a lack of sophisticated baseband modeling, the front-ends  $\mathbf{c}_{[T/R]B,i}$  can be assumed as allpass filters. Here, a fixed length of  $L_f = 16$  is chosen for the Tx and Rx chains, each having a frequency response magnitude of  $1 + \delta_i$  over the effective bandwidth, with  $\delta_i$  being a normally distributed mismatch parameter per sample at BS antenna  $i$  with fixed variance  $\sigma_\delta^2$ . This model is valid due to the original design target of the circuitry, which should have unit gains over the whole desired band and as little coupling effects as possible. With the assumptions in (7) we can write

$$\hat{\mathbf{h}}_{i,j}(t) = \hat{\mathbf{g}}_{j,i}(t) * \mathbf{c}_{B,i}(t), \quad (8)$$

with  $\mathbf{c}_{B,i}(t) = \mathcal{F}^{-1} \{ \mathbf{C}_{TB,i}(\Omega) \cdot \mathbf{C}_{RB,i}(\Omega) \}$ , where  $\mathcal{F}^{-1} \{ \cdot \}$  denotes the inverse Fourier transform operator and  $\Omega$  the frequency index [7]. Eq. (8) still assumes independency of the filters  $\mathbf{c}_{B,i}(t)$ , meaning no coupling effects are existent. In the following sections, we assume sampled versions of the impulse responses to account for different delay spreads and therefore different lengths of  $\hat{\mathbf{g}}_{i,j}(t)$  and  $\hat{\mathbf{h}}_{i,j}(t)$ . The lengths of the impulse responses directly determine the order of the optimization problem.

## III. CALIBRATION PRINCIPLES

To present the calibration approach, the STLS problem is initially derived. Afterwards, the proposed iterative algorithm is described.

### A. Derivation of the STLS Problem

Several principles for system calibration have been introduced in the past. The most popular ones in multi-antenna systems are absolute calibration with respect to a reference antenna or calibration by means of external reference sources. These sources may require additional hardware, which is undesired in most cases. In TDD the idea of relative calibration became interesting with more powerful signal processing and with the application of more complex adaptive schemes [7].

Since the relative calibration principle needs knowledge of the UL and DL channel, additional feedback of the DL channel

during UL transmission is required prior to the calibration process. This can be achieved, e.g., by means of analog feedback [19]. This feedback is required at the BS only once or in large intervals as the front-end characteristics may not change in time or their variations, e.g., due to temperature are much slower compared to the channel variations. Fig. 3 shows the idea of the workflow in the calibration procedure. As depicted, the time requirements  $\tau_C$  of the calibration are

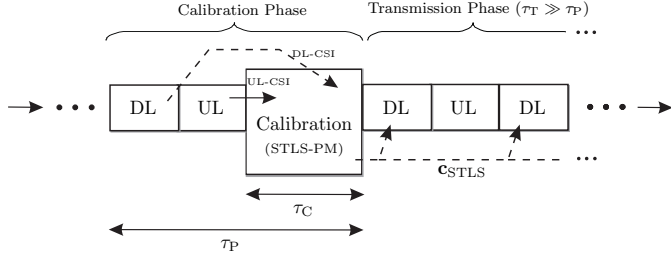


Fig. 3. Workflow of relative calibration procedure in time-domain

slackened as the transmission time  $\tau_T$  is usually much larger, even if an additional full duplex phase is used for feedback purposes and  $\tau_P > \tau_C$ . In the figure,  $\mathbf{c}_{\text{STLS}}$  is the solution vector of the optimization problem derived in the following, which subsequently can be used for calibration of the UL channel estimate to achieve a proper CSI of the instantaneous effective DL channel.

If the estimates of both the impulse responses  $\hat{\mathbf{g}}_{i,j}(t)$  and  $\hat{\mathbf{h}}_{i,j}(t)$  of all antenna pairs  $i, j$  are available at the BS in the calibration phase, (8) can be used to formulate a set of equations in matrix/vector notation neglecting time index  $t$ , e.g., for a  $2 \times 2$  system

$$\underbrace{\begin{bmatrix} \mathcal{T}\{\hat{\mathbf{g}}_{1,1}\} & \mathbf{0} & \mathbf{0} & \mathbf{0} \\ \mathbf{0} & \mathcal{T}\{\hat{\mathbf{g}}_{1,2}\} & \mathbf{0} & \mathbf{0} \\ \mathbf{0} & \mathbf{0} & \mathcal{T}\{\hat{\mathbf{g}}_{2,1}\} & \mathbf{0} \\ \mathbf{0} & \mathbf{0} & \mathbf{0} & \mathcal{T}\{\hat{\mathbf{g}}_{2,2}\} \end{bmatrix}}_{\mathbf{G}_C \in \mathbb{C}^{L_h N_B N_M \times L_c N_B N_M}} \underbrace{\begin{bmatrix} \mathbf{c}_{1,1} \\ \mathbf{c}_{1,2} \\ \mathbf{c}_{2,1} \\ \mathbf{c}_{2,2} \end{bmatrix}}_{\mathbf{c} \in \mathbb{C}^{L_h N_B N_M}} = \underbrace{\begin{bmatrix} \hat{\mathbf{h}}_{1,1} \\ \hat{\mathbf{h}}_{1,2} \\ \hat{\mathbf{h}}_{2,1} \\ \hat{\mathbf{h}}_{2,2} \end{bmatrix}}_{\mathbf{h} \in \mathbb{C}^{L_h N_B N_M}} \quad (9a)$$

$$\mathbf{G}_C \mathbf{c} = \mathbf{h}, \quad (9b)$$

where  $\mathcal{T}\{\cdot\}$  is the Toeplitz operator and  $\mathbf{c} \in \mathbb{C}^{L_c N_B N_M}$  is the desired solution vector of stacked impulse responses to calibrate the system, and  $L_c = L_g - L_h + 1$ . To ensure a sufficient length of the solution vector,  $L_c \geq L_f$  should be guaranteed, thus, for equal physical channel lengths, zero padding can be applied in (9) for the UL channel vectors. As a consequence, the length of the impulse responses must be chosen carefully to ensure a solution to (9). The existing block-diagonal structure of  $\mathbf{G}_C$  can be exploited by simply decomposing (9) into  $N_M$  single-filter equations due to the joint linear correspondence. It is worth to mention that a multiple application of the proposed algorithm can be parallelized, but may lead to different solutions of the individual filter vectors for different channel realizations as compared to the stacked formulation (9).

As both the observation vector  $\mathbf{h}$  and the parameter matrix  $\mathbf{G}_C$  in particular are disturbed by noise due to the channel estimation process and in addition the system is overdetermined, the intuitive least squares (LS) solution does not lead to a unique solution vector  $\mathbf{c}$  and the system equation should rather be expressed as  $\mathbf{G}_C \mathbf{c} \approx \mathbf{h}$  [20]. Instead, it was shown that the following total least squares (TLS) minimization problem

$$\underset{\Delta \mathbf{G}_C, \Delta \mathbf{h}}{\text{minimize}} \quad \|\Delta \mathbf{G}_C, \Delta \mathbf{h}\|_F \quad (10a)$$

$$\text{s.t.} \quad (\mathbf{G}_C + \Delta \mathbf{G}_C) \mathbf{c} = (\mathbf{h} + \Delta \mathbf{h}) \quad (10b)$$

leads to the *true* solution given by  $\mathbf{c} = \mathbf{G}_C^+ \mathbf{h}$  consistently as the number of rows in  $\mathbf{G}_C$  tend to infinity [20]. An even closer approximation to this solution can be achieved by overparameterization of (9). Therefore, simply multiple measurements of UL and DL channels can be used and the calibration time  $\tau_P$  is increased such that

$$\begin{bmatrix} \mathbf{G}_C(1) \\ \vdots \\ \mathbf{G}_C(K) \end{bmatrix} \mathbf{c} = \begin{bmatrix} \mathbf{h}(1) \\ \vdots \\ \mathbf{h}(K) \end{bmatrix}, \quad (11)$$

where  $K$  denotes the number of measurements used for calibration. Due to the initial claim that the influence of the front-ends at the MS is negligible in the BS pre-equalization approach no overparameterization as compared to [7] is required since the impulse responses are still jointly linear. Hence, we restrict ourselves to  $K = 1$ . Anyway, the exploitation of multiple channel measurements in the calibration process by overdetermining problem (10) leads to more accurate results but also dramatically increases the complexity of the problem.

With the additional constraint that the resulting augmented matrix  $[\hat{\mathbf{G}}_C, \hat{\mathbf{h}}] = [\mathbf{G}_C + \Delta \mathbf{G}_C, \mathbf{h} + \Delta \mathbf{h}]$  should have the same affine structure as  $[\mathbf{G}_C, \mathbf{h}]$ , (10) is called a structured TLS (STLS) problem. Its solution determines an augmented perturbation matrix  $[\Delta \mathbf{G}_C, \Delta \mathbf{h}]$  with minimum Frobenius norm that lowers the rank of the augmented matrix  $[\mathbf{G}_C, \mathbf{h}]$  while preserving the inherent special structure [7].

### B. Iterative Algorithm Based on Property Mapping

To obtain a solution to (10), we propose an iterative algorithm based on two fundamental mathematical properties. The first is predetermined by the fact that a TLS problem can be solved by the singular value decomposition (SVD). Consider the following decompositions

$$[\mathbf{G}_C, \mathbf{h}] = \mathbf{U} \Sigma \mathbf{V}^H = \mathbf{U} \begin{bmatrix} \sigma_1 & & \mathbf{0} \\ & \ddots & \\ \mathbf{0} & & \sigma_r \end{bmatrix} \mathbf{V}^H \quad (12a)$$

$$[\hat{\mathbf{G}}_C, \hat{\mathbf{h}}] = \mathbf{U} \hat{\Sigma} \mathbf{V}^H, \quad (12b)$$

with  $\hat{\Sigma} = \text{diag}\{\sigma_1, \dots, \sigma_k, 0\}$ , where  $r = k+1$  is the rank of  $[\mathbf{G}_C, \mathbf{h}]$ . Accordingly, the SVD is applied for approximating the matrix  $[\mathbf{G}_C, \mathbf{h}]$  by a matrix  $[\hat{\mathbf{G}}_C, \hat{\mathbf{h}}]$  of lower rank, where the null space of this solution comprises the right

most singular vector corresponding to the singular value, which is zero. This method is based on the Eckart-Young-Mirsky matrix approximation theorem, which states that the optimum reduction from rank  $r$  to rank  $k$  can be achieved with minimum change in norm by removing all singular triplets for  $i = k+1, \dots, r$ . This corresponds to an approach of setting all singular values  $\sigma_i$  from index  $k+1$  to zero [20]. Consequently, the TLS correction term  $[\Delta \mathbf{G}_C, \Delta \mathbf{h}]$  must have a rank of one.

The second fundamental property comes from the property mapping theorem by Cadzow [16]. This theorem is necessary to prevent the inherent structure in the afore-mentioned STLS problem, which still remains a matrix approximation problem but with the prerequisite of preventing the structures given by (9) *as close as possible*. Without loss of generality, the following descriptions are restricted to linearly structured matrices. According to this assumption, each linearly structured matrix  $\mathbf{X} \in \mathbb{C}^{m \times n}$  can be described by a parameter vector  $\mathbf{x} \in \mathbb{C}^{mn \times 1}$  and a characteristic invertible matrix  $\mathbf{A}$  that provides linear combinations of the elements in the parameter vector. The following equations give an example for a  $3 \times 2$  Toeplitz matrix, which depicts a small-scale problem similar to parts of matrix  $\mathbf{G}_C$ .

*Example:* Assume a matrix  $\mathbf{X} \in \mathbb{C}^{3 \times 2}$  and its column vector representation  $\mathbf{x} = \text{vec}\{\mathbf{X}\} \in \mathbb{C}^{6 \times 1}$  with the corresponding characteristic matrix  $\mathbf{A} \in \mathbb{F}_2^{6 \times 4}$  given by

$$\mathbf{X} = \begin{bmatrix} \theta_1 & \theta_2 \\ \theta_3 & \theta_1 \\ \theta_4 & \theta_3 \end{bmatrix} \Leftrightarrow \mathbf{x} = \begin{bmatrix} \theta_1 \\ \theta_3 \\ \theta_4 \\ \theta_2 \\ \theta_1 \\ \theta_3 \end{bmatrix} \quad (13a)$$

$$\mathbf{A}\boldsymbol{\theta} = \begin{bmatrix} 1 & 0 & 0 & 0 \\ 0 & 0 & 1 & 0 \\ 0 & 0 & 0 & 1 \\ 0 & 1 & 0 & 0 \\ 1 & 0 & 0 & 0 \\ 0 & 0 & 1 & 0 \end{bmatrix} \begin{bmatrix} \theta_1 \\ \theta_2 \\ \theta_3 \\ \theta_4 \end{bmatrix}. \quad (13b)$$

With the Toeplitz structure of  $\mathbf{X}$  and vector representation  $\mathbf{x}$  the expression  $\mathbf{x} = \mathbf{A}\boldsymbol{\theta}$  shows the equivalence of  $\mathbf{X}$  and  $\mathbf{x}$  by considering the ordering transformation matrix  $\mathbf{A}$  [16, Lemma 3].  $\square$

In the example, the  $\text{vec}\{\cdot\}$ -operator creates a column vector from a matrix by stacking the columns of a matrix. By generalizing the ordering transformation due to the isomorphic and bijective mapping of the vector spaces  $\mathbb{C}^{m \times n}$  and  $\mathbb{C}^{mn \times 1}$ , we obtain the following relations

$$\mathbf{x} = f(\mathbf{X}) \quad \text{and} \quad \mathbf{X} = f^{-1}(\mathbf{x}), \quad (14)$$

in which  $f(\cdot)$  denotes a linear reordering transformation function, which preserves the  $\ell_2$ - and Frobenius norms of  $\mathbf{x}$  and  $\mathbf{X}$  such that  $\|\mathbf{x}\|_2 = \|\mathbf{X}\|_F$ .

Then, it has been shown that an arbitrary matrix  $\mathbf{X}_A$  that lies closest to the matrix  $\mathbf{X}$  with respect to the Frobenius norm

of the matrix difference is given by the property mapping

$$\begin{aligned} \mathbf{X}_A &= F_A(\mathbf{X}) \\ &= f^{-1}\left(\mathbf{A}(\mathbf{A}^T \mathbf{A})^{-1} \mathbf{A}^T f(\mathbf{X})\right), \end{aligned} \quad (15)$$

where  $F_A$  is a continuous and closed point-to-point mapping, if  $\sigma_k \neq \sigma_{k+1}$  holds [16]. Furthermore, the vectors associated with both matrices follow (14) and correlate such that  $\mathbf{x}_A = \mathbf{A}(\mathbf{A}^T \mathbf{A})^{-1} \mathbf{A}^T \mathbf{x}$ . Cadzow showed that the projection operator  $\mathbf{A}(\mathbf{A}^T \mathbf{A})^{-1} \mathbf{A}^T$  has a null space  $\mathcal{N}(\mathbf{A}^T)$ , which leads to

$$\|\mathbf{X}_A\|_F = \|\mathbf{X}\|_F \quad (16)$$

as long as matrix  $\mathbf{X}$  lies in a closed convex linear matrix subspace generated by matrix  $\mathbf{A}$  [16].

Accordingly, with regard to (15) the mapping matrix  $\mathbf{S}$  will be introduced for solving (10) such that

$$[\mathbf{G}_C, \mathbf{h}]_S = \text{vec}^{-1}\left\{\mathbf{S}(\mathbf{S}^T \mathbf{S})^{-1} \mathbf{S}^T \cdot \text{vec}\{[\mathbf{G}_C, \mathbf{h}]\}\right\}, \quad (17)$$

where  $\text{vec}^{-1}\{\cdot\}$  is the corresponding inverse  $\text{vec}$ -operator, which now depicts the two-dimensional linear reordering transformation of the optimization problem. The sparse binary matrix  $\mathbf{S} \in \mathbb{F}_2^{L_c N_B N_M (L_c N_B N_M + 1) \times 2 N_B N_M L_h}$  provides the specific characteristic matrix of the augmented matrix that preserves the norms in the sense that  $\|\text{vec}\{[\mathbf{G}_C, \mathbf{h}]\|_2 = \|[\mathbf{G}_C, \mathbf{h}]\|_F$ . Using this presumption, the proposed algorithm as stated in Algorithm 1 is as follows. The SVD of the augmented matrix  $[\mathbf{G}_C, \mathbf{h}] = \mathbf{U}\boldsymbol{\Sigma}\mathbf{V}^H$  is computed and the smallest singular value in  $\boldsymbol{\Sigma}$  is set to zero. Afterwards, the augmented matrix is recalculated with the adjusted diagonal matrix  $\hat{\boldsymbol{\Sigma}}$  such that the estimate  $[\hat{\mathbf{G}}_C, \hat{\mathbf{h}}] = \mathbf{U}\hat{\boldsymbol{\Sigma}}\mathbf{V}^H$  is obtained. (17) is then used to re-map the vector  $\text{vec}\{[\hat{\mathbf{G}}_C, \hat{\mathbf{h}}]\}$  to the original structure as in  $[\mathbf{G}_C, \mathbf{h}]$ . Another SVD is computed to estimate the resulting smallest singular value. If this value is beyond a certain threshold, the algorithm stops and the total least squares solution provides an estimate of vector  $\mathbf{c}$  [9], [21]. Otherwise, the smallest singular value is again set to zero and the procedure is repeated until convergence or any stopping criterion is reached. We refer to this algorithm as STLS with property mapping (STLS-PM) in the following.

### C. Convergence Criteria

According to [16, Theorem 1], where it is specified that any signal sequence  $\mathbf{x}_k$  generated by the iterative mapping rule

$$\mathbf{x}_k \in f(\mathbf{x}_{k-1}) \quad \text{for} \quad k \geq 1 \quad (18)$$

where  $\mathbf{x}_0$  describes the original signal and is chosen to be the initial signal in the iterations, converges to a solution with an appropriate structural property as long as the mapping  $f(\cdot)$  is closed and distant reducing. The proof traces back to the global convergence theorem of Zangwill [22]. The given statement holds for all possible known sequences, especially for complex-valued matrices with the restriction that the singular values of the matrix satisfy  $\sigma_k \neq \sigma_{k+1}$ . Then, (15) determines the unique mapping with a new matrix of a rank lower or

---

**Algorithm 1** STLS Algorithm based on Property Mapping

---

**Require:** Augmented matrix  $[\mathbf{G}_C, \hat{\mathbf{h}}]$  and characteristic structure matrix  $\mathbf{S}$

1: Compute the SVD of  $[\mathbf{G}_C, \hat{\mathbf{h}}]$

$$[\mathbf{G}_C, \hat{\mathbf{h}}] = \mathbf{U}^{(\ell)} \mathbf{\Sigma}^{(\ell)} [\mathbf{V}^{(\ell)}]^H$$

2: Extract the smallest singular value of the augmented matrix

$$\sigma_r^{(\ell)} = \Sigma_{r,r}^{(\ell)}$$

3: **while**  $\sigma_r^{(\ell)} > \epsilon$  **and**  $\ell < \max.$  iterations **do**

4:      $\Sigma_{r,r}^{(\ell)} = 0$

5:     Compute adjusted matrix

$$[\hat{\mathbf{G}}_C^{(\ell+1)}, \hat{\mathbf{h}}^{(\ell+1)}] = \mathbf{U}^{(\ell)} \hat{\Sigma}^{(\ell)} [\mathbf{V}^{(\ell)}]^H$$

6:     Compute a structured matrix  $[\hat{\mathbf{G}}_C^{(\ell+1)}, \hat{\mathbf{h}}^{(\ell+1)}]_{\mathbf{S}}$  using the property mapping principle

$$[\hat{\mathbf{G}}_C^{(\ell+1)}, \hat{\mathbf{h}}^{(\ell+1)}]_{\mathbf{S}} = \text{vec}^{-1} \left\{ \mathbf{S} (\mathbf{S}^T \mathbf{S})^{-1} \mathbf{S}^T \text{vec} \left\{ [\hat{\mathbf{G}}_C^{(\ell+1)}, \hat{\mathbf{h}}^{(\ell+1)}] \right\} \right\}$$

7:     Recalculate the SVD of the structured matrix

$$[\hat{\mathbf{G}}_C^{(\ell+1)}, \hat{\mathbf{h}}^{(\ell+1)}]_{\mathbf{S}} = \mathbf{U}^{(\ell+1)} \mathbf{\Sigma}^{(\ell+1)} [\mathbf{V}^{(\ell+1)}]^H$$

8:      $\sigma_r^{(\ell+1)} = \Sigma_{r,r}^{(\ell+1)}$

9:      $\ell \leftarrow \ell + 1$

10: **end while**

11: **return**      $\mathbf{c}_{\text{STLS}} = -\frac{\mathbf{v}_{1:L_c \cdot N_B \cdot N_M, L_c \cdot N_B \cdot N_M + 1}^{(\ell)}}{v_{r,r}^{(\ell)}}$      **and**  
                   $[\hat{\mathbf{G}}_C^{(\ell)}, \hat{\mathbf{h}}^{(\ell)}]_{\mathbf{S}}$

---

equal to the original matrix and with closest distance in the Frobenius norm sense [16].

Results for the applied system model from Sec. II, which show the applicability and convergence of this algorithm, will now be presented.

#### IV. SIMULATION RESULTS

In this section, bit error rate (BER) results versus  $E_b/N_0$  for linear MMSE pre-equalization in a multi-user MISO single-carrier FDE scenario with  $N_B = 2$  BS antennas and  $N_M = 2$  non-cooperating single-antenna receivers applying a  $N_c = 256$  FFT-length and 16-QAM transmission are shown. There, the  $E_b/N_0$ -ratio is defined as  $E_b/N_0 = 1/(R_c \log_2(M) \sigma_N^2)$ , where  $R_c$  is the code rate of the applied channel code, which in the encoded scenarios is a half-rate punctured 3GPP Turbo Code with additional sub-block interleaving [23]. It is assumed that a codeword ranges over six frames, each frame consists of  $N_c$  QAM symbols per user. The utilized QAM soft output demapping is done via max-log approximation. The necessary cyclic prefix has a length of  $N_g = 32$ , which is set to be at least the length of the considered effective channels at symbol clock to avoid interference coming from a too short prefix. For completeness, it has to be mentioned that the guard loss is also considered in the results. The physical channel has an almost exponentially decaying power delay profile with a

strong second path according to the 3GPP SCM-A channel but shortened to  $L_p = 6$ . Furthermore, the channel is assumed to be constant for one codeword but changes from codeword to codeword. The MMSE predictor model for each the UL and DL channels provides a constant channel estimation error variance of  $\sigma_e^2 = 10^{-4}$ , which is assumed to be independent of the transmit power for simplicity. The error variance  $\sigma_\delta^2$  describing the non-reciprocity of the allpass filters varies during the simulations.

To initially show the convergence properties of the STLS-PM algorithm, Fig. 4 depicts the smallest singular value  $\sigma_r$  in each iteration  $\ell$  for an exemplary  $2 \times 2$  system with a fixed filter non-reciprocity variance of  $\sigma_\delta^2 = -30$  dB. The stopping criteria are chosen to  $\epsilon = 10^{-12}$  and a set maximum number of iterations of 10. These parameters also hold for the BER results. For this specific example the first stopping criteria is not fulfilled, hence, the full number of ten iterations is executed. Consequently, the descent-type principle of the algorithm is observable, while the changing channel estimation error variance results in an increase of  $\sigma_r$  at the beginning of the algorithm. After only a few iterations the algorithm achieves a decreased singular value, while preserving the structure of matrix  $[\hat{\mathbf{G}}_C, \hat{\mathbf{h}}]$ . If the augmented matrix has a large condition number and therefore has a very small  $\sigma_r$ , which is beyond the threshold  $\epsilon$ , it may happen that the STLS-PM solution coincides with the ordinary TLS solution as no iteration is executed. Thus, the behavior of the algorithm strongly depends on the properties of the augmented matrix and, hence, strongly depends on the length  $L_g$ , which should be presumed appropriate to avoid ill-conditioning.

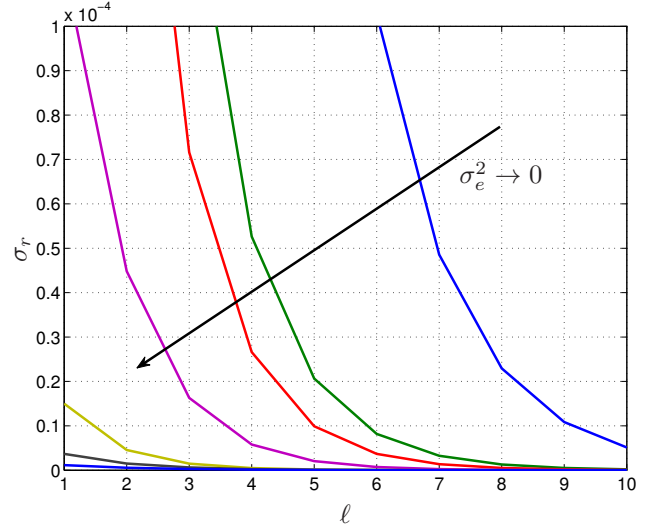


Fig. 4. Convergence of STLS-PM algorithm indicated by the smallest singular value  $\sigma_{k+1}$  versus the iteration number  $\ell$  for different channel estimation error variances  $\sigma_e^2 \in \{10^{-1}, 10^{-2}, \dots, 10^{-8}\}$ ; exemplary  $2 \times 2$  channel with  $\sigma_\delta^2 = -30$  dB

The resulting BER curves for uncoded transmission are depicted in Fig. 5. Different degrees of mismatch  $\sigma_\delta^2$  are shown. The results indicate error floors in case of uncalibrated

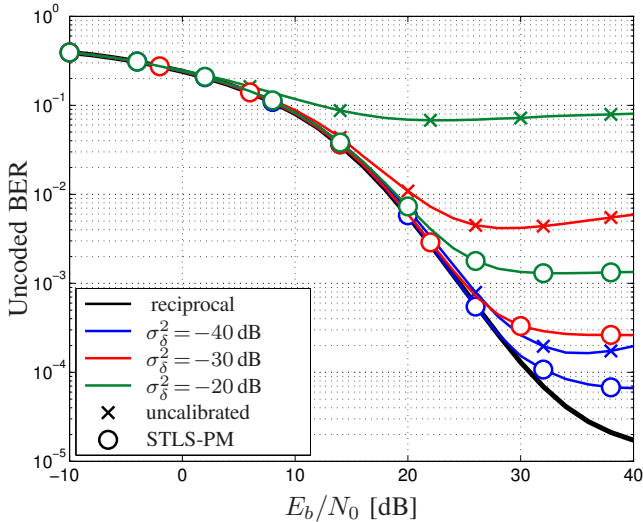


Fig. 5. Uncoded BER versus  $E_b/N_0$  for an uncalibrated and a calibrated SC-preFDE system with  $N_B = N_M = 2$ ,  $N_c = 256$ -FFT length and 16-QAM with linear MMSE pre-equalization and different reciprocity mismatch conditions; channel estimation error variance  $\sigma_e^2 = 10^{-4}$

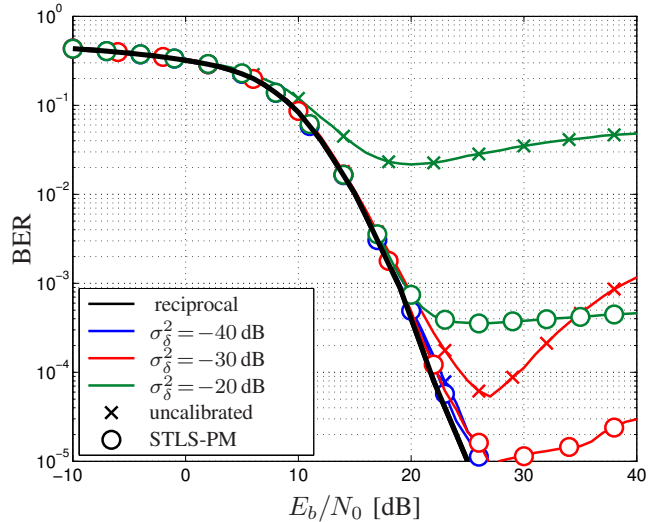


Fig. 6. Coded BER versus  $E_b/N_0$  for an uncalibrated and a calibrated SC-preFDE system with  $N_B = N_M = 2$ ,  $N_c = 256$ -FFT length and 16-QAM with linear MMSE pre-equalization and different reciprocity mismatch conditions; channel estimation error variance  $\sigma_e^2 = 10^{-4}$

systems- the larger the mismatch between the UL and DL chains based on  $\sigma_\delta^2$  the higher the error floor. The increasing BER curves correspond to the results in [9], where small noise powers lead to increased interference powers due to non-reciprocal Tx and Rx chains. Calibrating the system with the STLS-PM proves to decrease the error rates and avoids the afore-mentioned error rate increase. Especially in moderate to severe mismatch conditions the calibrated system can deal with differing RF chains at the BS. Thus, calibration is valuable if the frequency-responses of the BS chains are highly inconsistent in magnitude, are not compensated for in the design process of the BS or their mismatch strongly varies with time.

To additionally confirm the previous uncoded results, Fig. 6 shows the results for a scenario, where each MS applies the 3GPP Turbo encoder and soft-in/soft-out max-log-MAP Turbo decoding. As expected, in scenarios with slightly mismatched BS front-ends according to  $\sigma_\delta^2 = -40$  dB or  $\sigma_\delta^2 = -30$  dB the strong Turbo code can cope with the caused interference without additional signal processing. This is apparent at bit error rates of  $10^{-3}$ , which are established error rates considering coded scenarios. Nonetheless, in severe mismatch conditions according to  $\sigma_\delta^2 = -20$  dB even with channel coding a high error floor exists that can only be avoided by means of calibration. The STLS-PM algorithm almost achieves the optimum reciprocal case, with only a loss of 0.5 dB at a BER of  $10^{-3}$ . However, it was shown that the non-reciprocal transceiver chains have a higher influence on higher-order modulation [3]. As we restricted ourselves to 16-QAM, it can be concluded, that the application of such a calibration algorithm is of utmost importance with increasing demands in high-rate wireless adaptive systems even in small or moderate mismatch conditions.

## V. CONCLUSION

In this contribution the time-domain calibration using a structured total least squares approach based on signal property mapping principles for application in, e.g., SC-preFDE systems is presented. If noisy and mismatched UL and DL channel estimates are available at the BS in a special calibration phase the proposed STLS-PM approach can achieve excellent calibration results in terms of bit error rates, especially in severe mismatch conditions. In addition, the algorithm shows good convergence properties and makes efficient use of singular value decompositions. Due to the structure preserving principle, the algorithm is capable of dealing with a frequency-selective nature of wireless multi-user MISO channels.

Future research may include regularization of the total least squares approaches, also known as generalized TLS problems, to avoid singularities in the optimization problem and to achieve accelerated versions of the algorithm. The consideration of coupling effects, which destroy the joint linearity in the unknowns of the optimization problem, may also be investigated in the future.

## ACKNOWLEDGEMENTS

The authors like to thank Prof. Dr.-Ing. Georg Fischer from the Institute for Technical Electronics at the University of Erlangen-Nuremberg for the helpful discussions about RF components and reasonable front-end baseband modeling.

## REFERENCES

- [1] C. Degen, "Frequency-Domain Signal Processing for Space-Division Multiple Access with Consideration of Front-End Imperfections," PhD thesis, RWTH Aachen, Germany, July 2005.
- [2] W. Keusgen, "Antennenkonfiguration und Kalibrierungskonzepte für die Realisierung reziproker Mehrantennensysteme," PhD thesis (in German), RWTH Aachen, Germany, Oct. 2005.

- [3] R. Habendorf and G. Fettweis, "Pre-Equalization for TDD Systems with Imperfect Transceiver Calibration," in *IEEE Proc. Vehicular Technology Conference (VTC), Spring*, Marina Bay, Singapore, May 2008.
- [4] S. Han, L. Su, C. Yang, G. Wang, and M. Lei, "Robust Multiuser Precoder for Base Station Cooperative Transmission with Non-ideal Channel Reciprocity," in *IEEE Proc. Global Communications Conference (GLOBECOM)*, Miami, FL, USA, Dec. 2010.
- [5] G. Fettweis, M. Löhning, D. Petrovic, M. Windisch, P. Zillmann, and W. Rave, "Dirty RF: A New Paradigm," in *Proceedings of the 16th IEEE International Symposium On Personal, Indoor And Mobile Radio Communications (PIMRC)*, Berlin, Germany, Sept. 2005.
- [6] A. Bourdoux, B. Come, and N. Khaled, "Non-reciprocal Transceivers in OFDM/SDMA Systems: Impact and Mitigation," in *IEEE Radio and Wireless Conference (RAWCON)*, Boston, MA, USA, Aug. 2003, pp. 183–186.
- [7] M. Guillaud, "Transmission and Channel Modeling Techniques for Multiple-Antenna Communication Systems," PhD thesis, Ecole Nationale Supérieure des Telecommunications, Paris, France, July 2005.
- [8] M. Petermann, D. Wübben, and K.-D. Kammeyer, "Evaluation of Encoded MU-MISO-OFDM Systems in TDD Mode with Non-ideal Channel Reciprocity," in *8th International ITG Conference on Source and Channel Coding (SCC)*, Siegen, Germany, Jan. 2010.
- [9] M. Petermann, M. Stefer, D. Wübben, M. Schneider, and K.-D. Kammeyer, "Low-Complexity Calibration of Mutually Coupled Non-Reciprocal Multi-Antenna OFDM Transceivers," in *The 7th International Symposium on Wireless Comm. Systems (ISWCS)*, York, UK, Sept. 2010.
- [10] J.-C. Guey and L. D. Larsson, "Modeling and Evaluation of MIMO Systems Exploiting Channel Reciprocity in TDD Mode," in *IEEE Vehicular Technology Conference Fall (VTC)*, Los Angeles, CA, USA, Sept. 2004.
- [11] Y. Hara, Y. Yano, and H. Kubo, "Antenna Array Calibration Using Frequency Selection in OFDMA/TDD Systems," in *IEEE Global Telecommunications Conference (Globecom)*, New Orleans, LA, USA, Nov. 2008.
- [12] M. Guillaud, D. T. M. Stock, and R. Knopp, "A practical method for wireless channel reciprocity exploitation through relative calibration," in *International Symposium on Signal Processing and its Applications (ISSPA)*, Sydney, Australia, Aug. 2005.
- [13] P. Lemmerling, "Structured Total Least Squares: Analysis, Algorithms and Applications," PhD thesis, Katholieke Universiteit Leuven, Belgium, May 1999.
- [14] J. B. Rosen, H. Park, and J. Glick, "Total Least Norm Formulation and Solution for Structured Problems," *SIAM Journal on Matrix Analysis and Applications*, vol. 17, no. 1, pp. 110–126, 1996.
- [15] N. Mastronardi, P. Lemmerling, and S. Van Huffel, "Fast Structured Total Least Squares Algorithm for Solving the Basic Deconvolution Problem," *SIAM Journal on Matrix Analysis and Applications*, vol. 22, no. 2, pp. 533–553, 2000.
- [16] J. A. Cadzow, "Signal Enhancement - A Composite Property Mapping Algorithm," *IEEE Transactions on Acoustics, Speech, and Signal Processing*, vol. 36, no. 1, pp. 49–62, Jan. 1988.
- [17] Y. A. Felus and B. Schaffrin, "Performing Similarity Transformations Using the Error-in-Variables Model," in *American Society for Photogrammetry & Remote Sensing (ASPRS) Annual Conference*, Baltimore, MD, USA, Mar. 2005.
- [18] L. Choi and R. D. Murch, "A Transmit MIMO Scheme With Frequency Domain Pre-Equalization for Wireless Frequency Selective Channels," *IEEE Transactions on Wireless Communications*, vol. 3, no. 3, pp. 929–938, May 2004.
- [19] T. L. Marzetta and B. M. Hochwald, "Fast Transfer of Channel State Information in Wireless Systems," *IEEE Transactions on Signal Processing*, vol. 54, no. 4, pp. 1268–1278, Apr. 2006.
- [20] S. Van Huffel and J. Vandewalle, *The Total Least Squares Problem: Computational Aspects and Analysis*, Society for Industrial and Applied Mathematics (SIAM), Philadelphia, PA, USA, 1991.
- [21] G. H. Golub and C. F. Van Loan, "An Analysis of the Total Least Squares Problem," *SIAM Journal on Numerical Analysis*, vol. 17, no. 6, pp. 883–893, Dec. 1981.
- [22] W. Zangwill, *Nonlinear Programming: A Unified Approach*, Prentice Hall, Englewood Cliffs, NJ, USA, 1969.
- [23] 3GPP TSG RAN, "E-UTRA; Multiplexing and Channel Coding (Release 8)," Tech. Rep. 36.212 V8.7.0, 3GPP, May 2009.